Int. J. Heat Mass Transfer Vol. 33, No. 9, pp. 2019–2028, 1990
Printed in Great Britain

0017-9310/90 $3.00 + 0.00


# Non-parallel thermal instability of forced convection flow over a heated, non-isothermal horizontal flat plate

H. R. LEE, T. S. CHEN and B. F. ARMALY
Department of Mechanical and Aerospace Engineering and Engineering Mechanics, University of Missouri–Rolla, Rolla, MO 65401, U.S.A.

(*Received* 20 *April* 1989 *and in final form* 14 *November* 1989)

**Abstract**—A linear, non-parallel flow model is employed to study the onset of longitudinal vortex instability in laminar forced convection flow over a heated horizontal flat plate with variable surface temperature, $T_w(x) - T_\infty = Ax^n$. In the analysis, the streamwise dependence of the disturbance amplitude functions is taken into account. The resulting system of linearized disturbance equations for the amplitude functions constitutes an eigenvalue problem which is solved by a finite difference scheme along with Müller's shooting method. Neutral stability curves as well as the critical values for $Gr_x/Re_x^{3/2}$ and the corresponding critical wave numbers $\alpha^*$ are presented for Prandtl numbers $0.7 \leqslant Pr \leqslant 10^4$ over a range of the exponent $-0.5 \leqslant n \leqslant 1.0$. For a given Prandtl number, thermal instability is found to decrease as the value of the exponent $n$ increases. Also, for a given value of the exponent $n$, fluids with larger Prandtl numbers are found to exhibit less susceptibility to instability than fluids with lower Prandtl numbers. However, this latter trend exists for $Pr \leqslant 100$. For $Pr > 100$, the critical values of $Gr_x/Re_x^{3/2}$ become essentially constant and independent of the Prandtl number. The results from the present non-parallel flow analysis are also compared with available analytical and experimental results from previous studies. The non-parallel flow analysis that accounts for the streamwise dependence of the amplitude functions is found to have a stabilizing effect as compared to the parallel flow analysis in which streamwise dependence of the disturbance is neglected.

## INTRODUCTION

THE INSTABILITY of laminar boundary layer flows, due to either the wave mode or the vortex mode of instability, has been the subject of many studies. Instability of laminar forced convection flow over a horizontal, upward-facing heated plate, arising from the vortex mode of disturbance, was first analyzed by Wu and Cheng [1] using the linear stability theory. Moutsoglou *et al.* [2] also employed the linear theory to analyze the thermal instability of laminar mixed convection flow over a heated horizontal flat plate. In the latter study, the main flow and thermal fields were treated as non-parallel, but the disturbances were assumed to have the form of a stationary longitudinal vortex roll that is periodic in the spanwise direction. That is, the $x$-dependence of the disturbances was neglected. Recently, Chen and Chen [3] studied the vortex instability of laminar boundary layer flow over wedges by employing a non-parallel flow model that accounted for the streamwise dependence of the disturbances. Very recently, in re-examining the vortex instability of laminar forced convection flow over a heated horizontal flat plate, Yoo *et al.* [4] also considered the streamwise dependence of the disturbances and used the thermal boundary layer thickness as the reference length scale. Their analysis is good only for fluids with very large Prandtl numbers ($Pr \to \infty$) and solutions were obtained by power series. For this reason, their results are of limited practical utility.

In the present paper, vortex instability of laminar forced convection flow over a horizontal, upward-facing heated plate with the power-law variation in the surface temperature, $T_w(x) = T_\infty + Ax^n$, is examined for a wide range of Prandtl numbers, using the non-parallel flow model. The resulting eigenvalue problem for the disturbance amplitude functions was solved by an efficient finite difference method [5] in conjunction with Müller's shooting procedure.

Neutral stability curves as well as the critical values of $Gr_x/Re_x^{3/2}$ and the associated critical wave numbers were obtained for Prandtl numbers of 0.7, 7, $10^2$, $10^3$ and $10^4$ over a range of the exponent values $-0.5 \leqslant n \leqslant 1.0$.

## ANALYSIS

### *The main flow and thermal fields*

As the first step in the analysis of the vortex instability of the flow, attention is directed to the main flow and thermal fields. Consider laminar forced convection over a horizontal flat plate with its heated surface facing upward and its surface temperature varying as $T_w(x) = T_\infty + Ax^n$, where $A$ and $n$ are real constants and $T_\infty$ is the free stream temperature. The free stream velocity is $U_\infty$. The physical coordinates are chosen such that $x$ measures the streamwise distance from the leading edge of the plate and $y$ the distance normal to the plate. Under the assumption of constant fluid properties, the transformed system of the boundary layer equations governing the main

## NOMENCLATURE

$a$ dimensionless wave number of disturbances
$C_{fx}$ local friction factor, $\tau_w/(\rho U_\infty^2/2)$
$f$ reduced stream function, $\psi/(\nu U_\infty x)^{1/2}$
$g$ gravitational acceleration
$Gr_x$ local Grashof number, $g\beta[T_w(x)-T_\infty]x^3/\nu^2$
$Gr_L$ Grashof number based on $L$, $g\beta[T_w(L)-T_\infty]L^3/\nu^2$
$L$ characteristic length
$n$ exponent in the power-law variation of the wall temperature
$Nu_x$ local Nusselt number
$p'$ perturbation pressure
$P$ main flow pressure
$Pr$ Prandtl number
$Re_x$ local Reynolds number, $U_\infty x/\nu$
$Re_L$ Reynolds number based on $L$, $U_\infty L/\nu$
$t$ dimensionless amplitude function of temperature disturbance
$t'$ perturbation temperature
$T$ main flow temperature
$u, v, w$ dimensionless amplitude functions of velocity disturbance in the $x, y, z$ directions, respectively
$u', v', w'$ streamwise, normal, and spanwise components of perturbation velocity
$U, V$ streamwise and normal velocity components of main flow in the $x, y$ directions, respectively
$x, y, z$ streamwise, normal, and spanwise coordinates
$X, Y, Z$ dimensionless streamwise, normal, and spanwise coordinates, defined, respectively, as $x/L$, $y/\varepsilon L$, and $z/\varepsilon L$.

Greek symbols
$\alpha$ dimensionless wave number of disturbances, $aX^{1/2}$
$\tilde{\alpha}$ dimensionless wave number of disturbances based on thermal boundary layer thickness $\delta_t$
$\beta$ volumetric coefficient of thermal expansion
$\delta_m$ integral momentum boundary layer thickness
$\delta_t$ thermal boundary layer thickness
$\varepsilon$ dimensionless parameter, defined as $Re_L^{-1/2}$
$\eta$ similarity variable, $y(U_\infty/\nu x)^{1/2}$
$\theta$ dimensionless temperature, $(T-T_\infty)/[T_w(x)-T_\infty]$
$\kappa$ thermal diffusivity of fluid
$\nu$ kinematic viscosity of fluid
$\rho$ density of fluid
$\tau_w$ local wall shear stress
$\psi$ stream function.

Superscripts
$+$ dimensionless disturbance quantity
$-$ scale quantity defined by equation (20)
$*$ critical condition or dimensionless main flow quantity
$\hat{}$ resultant quantity.

Subscripts
w condition at the wall
0 dimensionless amplitude function
$\infty$ condition at the free stream.

flow and thermal fields can be expressed in dimensionless form as

$$f''' + \tfrac{1}{2} f f'' = 0 \tag{1}$$

$$\theta'' + \tfrac{1}{2} Pr\, f\theta' - n\, Pr\, f'\theta = 0 \tag{2}$$

$$f(0) = f'(0) = \theta(\infty) = 0, \quad f'(\infty) = \theta(0) = 1 \tag{3}$$

where the similarity variable $\eta(x, y)$, the reduced stream function $f(\eta)$, and the dimensionless temperature $\theta(\eta)$ are defined, respectively, as

$$\eta = y(U_\infty/\nu x)^{1/2}, \quad f(\eta) = \psi/(\nu U_\infty x)^{1/2},$$
$$\theta(\eta) = (T-T_\infty)/[T_w(x)-T_\infty]. \tag{4}$$

In equations (1)–(3), the primes denote derivatives with respect to $\eta$ and $Pr$ is the Prandtl number. Other notations are as defined in the Nomenclature.

Equations (1)–(3) were solved by a finite difference method in conjunction with the cubic spline interpolation scheme to provide the main flow quantities that are needed in the thermal instability calculations and to provide other physical quantities, such as the axial velocity profile $f'(\eta) = U/U_\infty$, the temperature profile $\theta(\eta)$, the local Nusselt number $Nu_x$, and the local friction factor $C_{fx}$. In terms of the dimensionless variables, the last two quantities can be expressed, respectively, by

$$Nu_x\, Re_x^{-1/2} = -\theta'(0), \quad C_{fx}\, Re_x^{1/2} = 2f''(0). \tag{5}$$

*Formulation of the stability problem*

In the present study, the linear stability theory is employed in the analysis. In experiments [6–9] the secondary flow vortex rolls have been found to be periodic in the spanwise direction. Thus, the disturbance quantities for velocity components $u', v', w'$, pressure $p'$, and temperature $t'$ are assumed to be functions of $(x, y, z)$. These disturbance quantities are superimposed on the two-dimensional main flow

quantities $U$, $V$, $W=0$, $P$, and $T$ to obtain the resultant quantities $\hat{U}$, $\hat{V}$, $\hat{W}$, $\hat{P}$, and $\hat{T}$ as follows:

$$\begin{aligned}\hat{U}(x,y,z) &= U(x,y)+u'(x,y,z)\\ \hat{V}(x,y,z) &= V(x,y)+v'(x,y,z)\\ \hat{W}(x,y,z) &= w'(x,y,z)\\ \hat{P}(x,y,z) &= P(x,y)+p'(x,y,z)\\ \hat{T}(x,y,z) &= T(x,y)+t'(x,y,z).\end{aligned} \tag{6}$$

The resultant quantities given by equation (6) satisfy the continuity equation, the Navier–Stokes equations, and the energy equation for an incompressible, three-dimensional steady fluid flow. Substituting equation (6) into these equations, subtracting the two-dimensional main flow, and linearizing the disturbance quantities, one can arrive at the following disturbance equations:

$$\frac{\partial u'}{\partial x}+\frac{\partial v'}{\partial y}+\frac{\partial w'}{\partial z}=0 \tag{7}$$

$$u'\frac{\partial U}{\partial x}+U\frac{\partial u'}{\partial x}+v'\frac{\partial U}{\partial y}+V\frac{\partial u'}{\partial y}=-\frac{1}{\rho}\frac{\partial p'}{\partial x}+\nu\nabla^2 u' \tag{8}$$

$$u'\frac{\partial V}{\partial x}+U\frac{\partial v'}{\partial x}+v'\frac{\partial V}{\partial y}+V\frac{\partial v'}{\partial y}=-\frac{1}{\rho}\frac{\partial p'}{\partial y}+\nu\nabla^2 v'+g\beta t' \tag{9}$$

$$U\frac{\partial w'}{\partial x}+V\frac{\partial w'}{\partial y}=-\frac{1}{\rho}\frac{\partial p'}{\partial z}+\nu\nabla^2 w' \tag{10}$$

$$u'\frac{\partial T}{\partial x}+U\frac{\partial t'}{\partial x}+v'\frac{\partial T}{\partial y}+V\frac{\partial t'}{\partial y}=\kappa\nabla^2 t' \tag{11}$$

where $\nabla^2=\partial^2/\partial x^2+\partial^2/\partial y^2+\partial^2/\partial z^2$ is the Laplacian operator.

Since the disturbances are confined within the boundary layer of the main flow, the so-called bottling effect by Haaland and Sparrow [10], the disturbances will have length scales different from those of the main flow field [11, 12]. To verify this, the disturbance equations are first nondimensionalized by using the length and velocity scales of the main flow. The coordinates are scaled as

$$X=\frac{x}{L},\quad Y=\frac{y}{\varepsilon L},\quad \text{and}\quad Z=\frac{z}{\varepsilon L} \tag{12}$$

where $\varepsilon=Re_L^{-1/2}$ and $Re_L=U_\infty L/\nu$ is the Reynolds number based on a characteristic length $L(x)$. If $L=x$, then $Y=\eta$ and $Re_L=Re_x$. Other main flow quantities are scaled as

$$U^*=\frac{U}{U_\infty},\quad V^*=\frac{V}{\varepsilon U_\infty},\quad \theta=\frac{T-T_\infty}{T_w(x)-T_\infty} \tag{13}$$

where $U^*$, $V^*$, and $\theta$ and their derivatives with respect to $X$ and $Y$ are of the order of 1. Similarly, the disturbance quantities can be scaled as

$$u^+=\frac{u'}{U_\infty},\quad v^+=\frac{v'}{U_\infty},\quad w^+=\frac{w'}{U_\infty},$$

$$p^+=\frac{p'}{\rho U_\infty^2\varepsilon}=\frac{p'Re_L^{1/2}}{\rho U_\infty^2},\quad t^+=\frac{t'}{T_w(x)-T_\infty} \tag{14}$$

where $u^+$, $v^+$, $w^+$, $p^+$, and $t^+$ and their derivatives with respect to $X$ and $Y$ are of the order of $\varepsilon$.

Substituting the above dimensionless variables from equations (12)–(14) into equations (7)–(11), one arrives at

$$\varepsilon\frac{\partial u^+}{\partial X}+\frac{\partial v^+}{\partial Y}+\frac{\partial w^+}{\partial Z}=0 \tag{15}$$

$$u^+\frac{\partial U^*}{\partial X}+U^*\frac{\partial u^+}{\partial X}+\frac{v^+}{\varepsilon}\frac{\partial U^*}{\partial Y}+V^*\frac{\partial u^+}{\partial Y}=-\varepsilon\frac{\partial p^+}{\partial X}+\varepsilon^2\frac{\partial^2 u^+}{\partial X^2}+\frac{\partial^2 u^+}{\partial Y^2}+\frac{\partial^2 u^+}{\partial Z^2} \tag{16}$$

$$\varepsilon u^+\frac{\partial V^*}{\partial X}+U^*\frac{\partial v^+}{\partial X}+v^+\frac{\partial V^*}{\partial Y}+V^*\frac{\partial v^+}{\partial Y}=-\frac{\partial p^+}{\partial Y}+\varepsilon^2\frac{\partial^2 v^+}{\partial X^2}+\frac{\partial^2 v^+}{\partial Y^2}+\frac{\partial^2 v^+}{\partial Z^2}+\frac{Gr_L}{Re_L^2}t^+ \tag{17}$$

$$U^*\frac{\partial w^+}{\partial X}+V^*\frac{\partial w^+}{\partial Y}=-\frac{\partial p^+}{\partial Z}+\varepsilon^2\frac{\partial^2 w^+}{\partial X^2}+\frac{\partial^2 w^+}{\partial Y^2}+\frac{\partial^2 w^+}{\partial Z^2} \tag{18}$$

$$u^+\frac{\partial\theta}{\partial X}+U^*\frac{\partial t^+}{\partial X}+\frac{v^+}{\varepsilon}\frac{\partial\theta}{\partial Y}+V^*\frac{\partial t^+}{\partial Y}=\frac{1}{Pr}\left(\varepsilon^2\frac{\partial^2 t^+}{\partial X^2}+\frac{\partial^2 t^+}{\partial Y^2}+\frac{\partial^2 t^+}{\partial Z^2}\right) \tag{19}$$

where $Re_L=U_\infty L/\nu$ is the Reynolds number and $Gr_L=g\beta[T_w(L)-T_\infty]L^3/\nu^2$ is the Grashof number based on the characteristic length $L$. Furthermore, since $Gr_L/Re_L^2$ is of the order of 1 and $Re_L$ is of the order of $\varepsilon^{-2}$, $Gr_L$ is of the order of $\varepsilon^{-4}$.

It is important to note that the term $(v^+/\varepsilon)\partial U^*/\partial Y$ in equation (16) and the term $(v^+/\varepsilon)\partial\theta/\partial Y$ in equation (19) are larger than other terms in the corresponding equation by at least an order of $(1/\varepsilon)$. This means that the $(X, Y, Z)$ variables as defined in equation (12) are not the appropriate length scales for the disturbances. Thus, by rescaling the coordinates for disturbance quantities along with the disturbance pressure in the form

$$(\bar{X},\bar{Y},\bar{Z},\bar{p}^+)=(X,Y,Z,p^+)\varepsilon^{-1/2} \tag{20}$$

one has

$$\varepsilon\frac{\partial u^+}{\partial\bar{X}}+\frac{\partial v^+}{\partial\bar{Y}}+\frac{\partial w^+}{\partial\bar{Z}}=0 \tag{21}$$

$$\varepsilon u^+\frac{\partial U^*}{\partial\bar{X}}+\varepsilon^{1/2}U^*\frac{\partial u^+}{\partial\bar{X}}+v^+\frac{\partial U^*}{\partial Y}+\varepsilon^{1/2}V^*\frac{\partial u^+}{\partial\bar{Y}}=-\varepsilon^2\frac{\partial\bar{p}^+}{\partial\bar{X}}+\varepsilon^2\frac{\partial^2 u^+}{\partial\bar{X}^2}+\frac{\partial^2 u^+}{\partial\bar{Y}^2}+\frac{\partial^2 u^+}{\partial\bar{Z}^2} \tag{22}$$

$$\varepsilon^2 u^+ \frac{\partial V^*}{\partial X} + \varepsilon^{1/2} U^* \frac{\partial v^+}{\partial \bar{X}} + \varepsilon v^+ \frac{\partial V^*}{\partial Y} + \varepsilon^{1/2} V^* \frac{\partial v^+}{\partial \bar{Y}}$$

$$= -\varepsilon \frac{\partial \bar{p}^+}{\partial \bar{Y}} + \varepsilon^2 \frac{\partial^2 v^+}{\partial \bar{X}^2} + \frac{\partial^2 v^+}{\partial \bar{Y}^2} + \frac{\partial^2 v^+}{\partial \bar{Z}^2} + \varepsilon \frac{Gr_L}{Re_L^2} t^+ \quad (23)$$

$$\varepsilon^{1/2} U^* \frac{\partial w^+}{\partial \bar{X}} + \varepsilon^{1/2} V^* \frac{\partial w^+}{\partial \bar{Y}}$$

$$= -\varepsilon \frac{\partial \bar{p}^+}{\partial \bar{Z}} + \varepsilon^2 \frac{\partial^2 w^+}{\partial \bar{X}^2} + \frac{\partial^2 w^+}{\partial \bar{Y}^2} + \frac{\partial^2 w^+}{\partial \bar{Z}^2} \quad (24)$$

$$\varepsilon u^+ \frac{\partial \theta}{\partial X} + \varepsilon^{1/2} U^* \frac{\partial t^+}{\partial \bar{X}} + v^+ \frac{\partial \theta}{\partial Y} + \varepsilon^{1/2} V^* \frac{\partial t^+}{\partial \bar{Y}}$$

$$= \frac{1}{Pr}\left(\varepsilon^2 \frac{\partial^2 t^+}{\partial \bar{X}^2} + \frac{\partial^2 t^+}{\partial \bar{Y}^2} + \frac{\partial^2 t^+}{\partial \bar{Z}^2}\right). \quad (25)$$

Since the terms $\varepsilon\ \partial u^+/\partial \bar{X}$, $\varepsilon^2\ \partial \bar{p}^+/\partial \bar{X}$, $\varepsilon^2\ \partial^2 u^+/\partial \bar{X}^2$, $\varepsilon^2\ \partial^2 v^+/\partial \bar{X}^2$, $\varepsilon^2\ \partial^2 w^+/\partial \bar{X}^2$, and $\varepsilon^2\ \partial^2 t^+/\partial \bar{X}^2$ in equations (21)–(25) are smaller than the rest of the terms in their respective equations, these terms can be omitted. The omission of these lowest order terms in the disturbance equations is consistent with the level of approximation of the main flow. With the above-mentioned terms deleted and by making use of equation (20), the disturbance equations reduce to

$$\frac{\partial v^+}{\partial Y} + \frac{\partial w^+}{\partial Z} = 0 \quad (26)$$

$$u^+ \frac{\partial U^*}{\partial X} + U^* \frac{\partial u^+}{\partial X} + Re_L^{1/2} v^+ \frac{\partial U^*}{\partial Y} + V^* \frac{\partial u^+}{\partial Y}$$

$$= \frac{\partial^2 u^+}{\partial Y^2} + \frac{\partial^2 u^+}{\partial Z^2} \quad (27)$$

$$Re_L^{-1/2} u^+ \frac{\partial V^*}{\partial X} + U^* \frac{\partial v^+}{\partial X} + v^+ \frac{\partial V^*}{\partial Y} + V^* \frac{\partial v^+}{\partial Y}$$

$$= -\frac{\partial p^+}{\partial Y} + \frac{\partial^2 v^+}{\partial Y^2} + \frac{\partial^2 v^+}{\partial Z^2} + \frac{Gr_L}{Re_L^2} t^+ \quad (28)$$

$$U^* \frac{\partial w^+}{\partial X} + V^* \frac{\partial w^+}{\partial Y} = -\frac{\partial p^+}{\partial Z} + \frac{\partial^2 w^+}{\partial Y^2} + \frac{\partial^2 w^+}{\partial Z^2} \quad (29)$$

$$u^+ \frac{\partial \theta}{\partial X} + U^* \frac{\partial t^+}{\partial X} + Re_L^{1/2} v^+ \frac{\partial \theta}{\partial Y} + V^* \frac{\partial t^+}{\partial Y}$$

$$= \frac{1}{Pr}\left(\frac{\partial^2 t^+}{\partial Y^2} + \frac{\partial^2 t^+}{\partial Z^2}\right). \quad (30)$$

Note that the main flow quantities, such as $U^*$, $\partial U^*/\partial X$, $\partial U^*/\partial Y$, $V^*$, $\partial V^*/\partial X$, $\partial V^*/\partial Y$, $\partial\theta/\partial X$, and $\partial\theta/\partial Y$, can be expressed in terms of $f(\eta)$, $\theta(\eta)$ and their $\eta$ derivatives. For example, $U^* = f'(\eta)$, $V^* = -X^{-1/2}[f(\eta) - \eta f'(\eta)]/2$, and $\partial\theta/\partial Y = X^{-1/2}\theta'(\eta)$.

Next, the pressure terms in equations (28) and (29) are eliminated by cross differentiation and subtraction. The resulting equation is then differentiated with respect to $Z$ once and the substitution $\partial w^+/\partial Z = -\partial v^+/\partial Y$ from the continuity equation is employed to remove the terms involving the function $w^+$ and its derivatives. This operation will yield three equations for the disturbance quantities $u^+$, $v^+$, and $t^+$. For the non-parallel flow model considered here, these quantities are expressed as

$$(u^+, v^+, t^+) = [u_0(X, Y), v_0(X, Y), t_0(X, Y)] \exp(i\alpha Z) \quad (31)$$

where $\alpha$ is the dimensionless azimuthal wave number of the disturbances. That is, the longitudinal vortex rolls are taken to be periodic in the spanwise $Z$-direction, with the amplitude functions depending on $X$ and $Y$.

Substituting equation (31) into equation (27), the combined form of equations (28) and (29) as described above, and equation (30), and letting

$$\alpha^2 = a^2 X, \quad u = u_0, \quad v = v_0 Re_x^{1/2}, \quad t = t_0 \quad (32)$$

one arrives at the following system of partial differential equations for the disturbance amplitude functions $u$, $v$, and $t$:

$$\mathrm{D}^2 u + a_1^* \mathrm{D}u + a_2^* u + a_3^* v = f' X \frac{\partial u}{\partial X} \quad (33)$$

$$\mathrm{D}^4 v + b_1^* \mathrm{D}^3 v + b_2^* \mathrm{D}^2 v + b_3^* \mathrm{D}v + b_4^* v + b_5^* u + b_8^* t$$

$$= f' X \frac{\partial}{\partial X}(\mathrm{D}^2 v) + f'' X \frac{\partial}{\partial X}(\mathrm{D}v) - f' \alpha^2 X \frac{\partial v}{\partial X} \quad (34)$$

$$\mathrm{D}^2 t + d_1^* \mathrm{D}t + d_2^* t + d_3^* u + d_4^* v = Pr\, f' X \frac{\partial t}{\partial X} \quad (35)$$

with boundary conditions

$$u = v = \mathrm{D}v = t = 0 \quad \text{at } \eta = 0 \quad \text{and} \quad \infty \quad (36)$$

where

$$a_1^* = \tfrac{1}{2}(f - \eta f'), \quad a_2^* = \tfrac{1}{2}\eta f'' - \alpha^2, \quad a_3^* = -f'',$$

$$b_1^* = \tfrac{1}{2}(f - \eta f'), \quad b_2^* = \tfrac{3}{2} f' - \tfrac{1}{2}\eta f'' - 2\alpha^2,$$

$$b_3^* = f'' - \tfrac{1}{2}\alpha^2 (f - \eta f'), \quad b_4^* = \alpha^4 + \tfrac{1}{2}\alpha^2(\eta f'' - f'),$$

$$b_5^* = \tfrac{1}{4}\alpha^2 (f - \eta f' - \eta^2 f''), \quad b_8^* = -\alpha^2 (Gr_x / Re_x^{3/2}),$$

$$d_1^* = \tfrac{1}{2} Pr\,(f - \eta f'), \quad d_2^* = -\alpha^2,$$

$$d_3^* = \tfrac{1}{2} Pr\, \eta\theta', \quad d_4^* = -Pr\,\theta' \quad (37)$$

in which $f$ and $\theta$ and their derivatives with respect to $\eta$ are from solutions of equations (1)–(3).

Equations (33)–(35) are partial differential equations and $\mathrm{D}^k$ stands for the $k$th partial differentiation with respect to $\eta$. The boundary conditions, equation (36), arise from the fact that the disturbances vanish at the wall and in the free stream. The condition $\mathrm{D}v = 0$ results from the continuity equation (26) along with $w = 0$ at $\eta = 0$ and $\infty$. These boundary conditions, however, are not sufficient for equations (33)–(35) if the $X$ derivatives of $u$, $v$, and $t$ are not to be set arbitrarily equal to zero. For weak $X$ dependence, $\partial/\partial X \ll \partial/\partial\eta$ and the terms on the right-hand side of equations (33)–(35) can be deleted or 'truncated'. This results in a system of equations for the 'local similarity' solution method, that resembles closely the system of equations for the case of the parallel flow model

in which the amplitude functions $u$, $v$, and $t$ depend only on the $Y$ or $\eta$ coordinate.

To define the problem completely, one needs to specify the initial conditions for $u$, $v$, and $t$ at an upstream location $X = X_1$. However, for the problem considered here, the terms involving $X\,\partial/\partial X$ can be replaced with $\eta\,\partial/\partial\eta$ by the coordinate transformation

$$X\frac{\partial}{\partial X} = X\frac{\partial}{\partial \eta}\frac{\partial \eta}{\partial X} = -\frac{1}{2}\eta\frac{\partial}{\partial \eta}. \tag{38}$$

With this transformation, equations (33)–(35) can be reduced to the following system of 'ordinary differential equations':

$$\mathrm{D}^2u + a_1\,\mathrm{D}u + a_2u + a_3v = 0 \tag{39}$$

$$\mathrm{D}^4v + b_1\,\mathrm{D}^3v + b_2\,\mathrm{D}^2v + b_3\,\mathrm{D}v + b_4v + b_5u + b_6t = 0 \tag{40}$$

$$\mathrm{D}^2t + d_1\,\mathrm{D}t + d_2t + d_3u + d_4v = 0 \tag{41}$$

along with the same boundary conditions as given by equation (36). The coefficients in equations (39)–(41) are

$$\begin{aligned} &a_1 = \tfrac{1}{2}f, \quad a_2 = a_2^*, \quad a_3 = a_3^* \\ &b_1 = \tfrac{1}{2}f, \quad b_2 = \tfrac{3}{2}f' - 2\alpha^2, \quad b_3 = f'' - \tfrac{1}{2}\alpha^2 f \\ &b_4 = b_4^*, \quad b_5 = b_5^*, \quad b_6 = b_6^* \\ &d_1 = \tfrac{1}{2}Prf, \quad d_2 = d_2^*, \quad d_3 = d_3^*, \quad d_4 = d_4^*. \end{aligned} \tag{42}$$

The system of coupled differential equations, equations (39)–(41), along with the boundary conditions, equation (36), constitutes an eigenvalue problem of the form

$$E(\alpha, Gr_x/Re_x^{3/2}; Pr, n) = 0. \tag{43}$$

For given values of the exponent $n$ and the Prandtl number $Pr$, the value of $Gr_x/Re_x^{3/2}$ satisfying equation (43) is sought as the eigenvalue for a prescribed value of the wave number $\alpha$.

## NUMERICAL METHOD OF SOLUTIONS

The system of equations for the main flow and thermal fields, equations (1)–(3), was solved by a finite difference scheme in conjunction with a cubic spline interpolation method similar to, but modified from that described in ref. [5] to provide the main flow quantities $f$, $f'$, $f''$, $\theta$, and $\theta'$ that are needed in the stability computation as well as in the determination of the local Nusselt number and the local friction factor. To conserve space, the details of the finite difference method of solution are omitted here. The stability problem, equations (39)–(41) and (36), was solved by a finite difference scheme along with Müller's shooting method, which parallels those described in ref. [5] and is also not repeated here. It suffices to mention some of its highlights. Equations (2) and (41) will become stiff when the Prandtl number is large. To solve stiff differential equations by the finite difference method, an upwind scheme or its equivalent is required. In the present study a finite difference method based on a weighting factor [5] is used which enables the numerical scheme to shift automatically from the central difference algorithm to the upwind difference algorithm, and vice versa. Also, to proceed with the numerical calculation of the stability problem, the boundary conditions at $\eta = \eta_\infty$ need to be approximated by the asymptotic solutions of equations (39)–(41) at $\eta = \eta_\infty$ (i.e. at the edge of the boundary layer). Since $f'' = \theta = \theta' = 0$ at $\eta = \eta_\infty$, the asymptotic solutions for $u$, $v$, and $t$ at $\eta = \eta_\infty$ can be obtained as

$$\begin{aligned} &u_2 = \exp(-m\eta_\infty), \quad u_1 = u_3 = u_4 = 0, \\ &v_1 = \exp(-\alpha\eta_\infty), \quad v_2 = \exp(-m\eta_\infty), \\ &v_3 = \exp(-r\eta_\infty), \quad v_4 = \exp(-b\eta_\infty), \\ &t_3 = \exp(-r\eta_\infty), \quad t_1 = t_2 = t_4 = 0 \end{aligned} \tag{44}$$

where

$$\begin{aligned} r &= \{-Pr\,C_1 + [(Pr\,C_1)^2 + 4\alpha^2]^{1/2}\}/2 \\ m &= \{-C_1 + [C_1^2 + 4\alpha^2]^{1/2}\}/2 \\ b &= \{-C_1 + [C_1^2 + 4(\alpha^2 - f'/2)]^{1/2}\}/2 \end{aligned} \tag{45}$$

with $C_1 = -f/2$. At any $\eta$ location, the solutions for $u$, $v$, and $t$ are

$$\begin{aligned} u(\eta) &= K_1u_1(\eta) + K_2u_2(\eta) + K_3u_3(\eta) + K_4u_4(\eta) \\ v(\eta) &= K_1v_1(\eta) + K_2v_2(\eta) + K_3v_3(\eta) + K_4v_4(\eta) \\ t(\eta) &= K_1t_1(\eta) + K_2t_2(\eta) + K_3t_3(\eta) + K_4t_4(\eta) \end{aligned} \tag{46}$$

where $K_1$, $K_2$, $K_3$, and $K_4$ are constants.

With a preassigned value of the exponent $n$, the main flow solution is first obtained for a fixed Prandtl number, $Pr$. Next, with the wave number $\alpha$ specified and the guessed value of $Gr_x/Re_x^{3/2}$, the finite difference form of equations (39)–(41) and (36) is numerically solved from $\eta = 0$ to $\eta_\infty$, ending with the asymptotic solutions for $u$, $v$, and $t$ at $\eta = \eta_\infty$. The correction for the value of $Gr_x/Re_x^{3/2}$ is then made by Müller's shooting method until the boundary conditions at the wall ($\eta = 0$) are satisfied within a certain specified tolerance [2]. This yields a converged value of $Gr_x/Re_x^{3/2}$ as the eigenvalue for given values of $n$, $Pr$, and $\alpha$.

After some experiments with the numerical solution, a step size of $\Delta\eta = 0.005$ and a value of $\eta_\infty = 10$ were found to be sufficient for both the main flow and the stability calculations for $Pr = 10^2$, $10^3$, and $10^4$. However, for $Pr = 0.7$ and 7, a step size of $\Delta\eta = 0.005$ and a value of $\eta_\infty = 20$ were needed to provide accurate numerical results for both. It is also of worth noting that a smaller step size $\Delta\eta$ is found to be more important than a larger value of $\eta_\infty$ for the accuracy of the numerical computations, especially when the wave number $\alpha$ is small.

## RESULTS AND DISCUSSION

To determine the stability and instability domains and the minimum value of $Gr_x/Re_x^{3/2}$ for the first onset of the vortex instability under various values of the exponent $n$ and the Prandtl number $Pr$, neutral stability curves (i.e. the $Gr_x/Re_x^{3/2}$ vs wave number curves) as well as the critical values of $Gr_x/Re_x^{3/2}$ and the corresponding critical wave number were obtained. Neutral stability curves for $0.7 \leqslant Pr \leqslant 10^3$ are plotted in Fig. 1 for exponent $n = 0$ (which is the uniform wall temperature case, UWT) and in Fig. 2 for $n = 0.5$ (which corresponds to the uniform surface heat flux case, UHF). It can be seen from these figures that as the Prandtl number increases the neutral stability curves shift right-upward to larger values of the wave number and $Gr_x/Re_x^{3/2}$. That is, the flow will become less susceptible to the vortex mode of instability as the Prandtl number increases. In addition, it can be observed that the larger the Prandtl number, the larger is the critical wave number, $\alpha^*$.

Figures 3–7 show the effect of the exponent $n$ on the neutral stability curves for various Prandtl numbers between 0.7 and $10^4$. It can be seen from these figures that for a given Prandtl number, the neutral stability curve shifts upward with increasing value of the exponent $n$. That is, the flow becomes less susceptible to the vortex mode of instability as the value of the exponent $n$ increases.

The critical values of $Gr_x/Re_x^{3/2}$ denoted by $G^*$ and

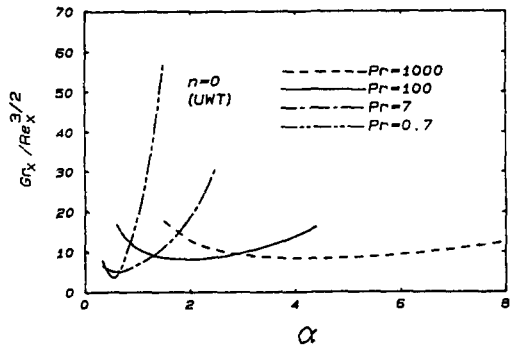


FIG. 1. Neutral stability curves for $n = 0$ (UWT).

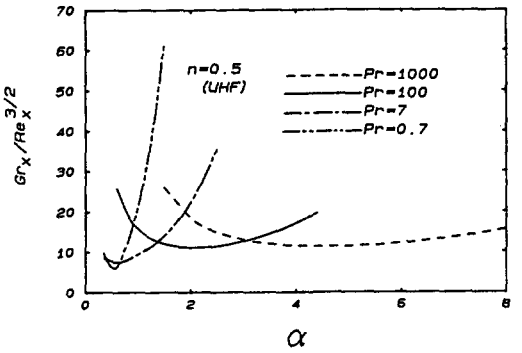


FIG. 2. Neutral stability curves for $n = 0.5$ (UHF).

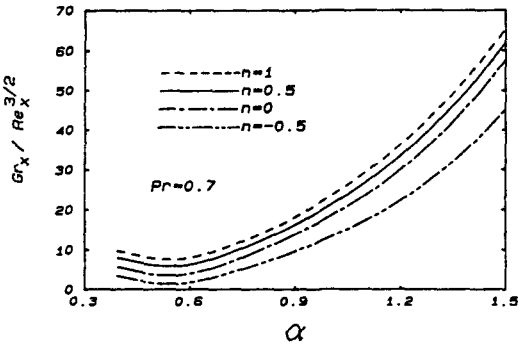


FIG. 3. The effect of $n$ on the neutral stability curves for $Pr = 0.7$

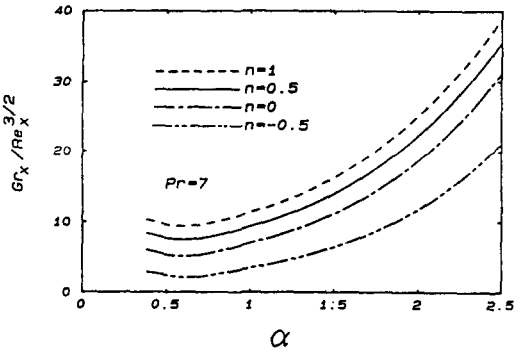


FIG. 4. The effect of $n$ on the neutral stability curves for $Pr = 7$.

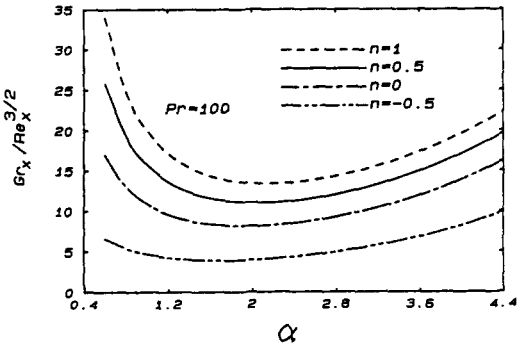


FIG. 5. The effect of $n$ on the neutral stability curves for $Pr = 100$.

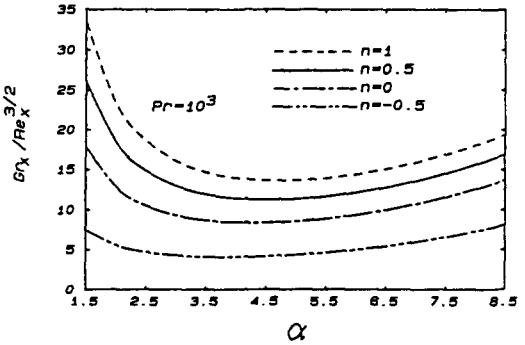


FIG. 6. The effect of $n$ on the neutral stability curves for $Pr = 1000$.

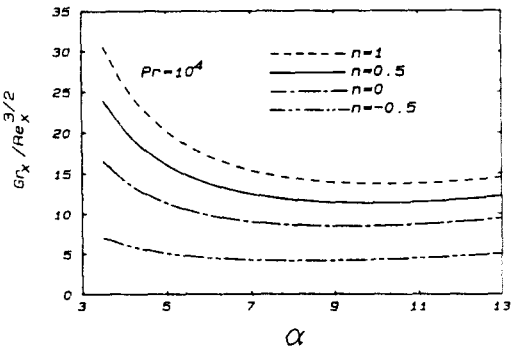


FIG. 7. The effect of $n$ on the neutral stability curves for $Pr = 10\,000$.

the corresponding critical wave number $\alpha^*$ from the present calculations for the different values of $n$ and $Pr$ are listed in Table 1. From Table 1, it can be seen that for a given Prandtl number $Pr$ the critical values of $Gr_x/Re_x^{3/2}$ for $n > 0$ are larger than that for the case of $n = 0$ (uniform wall temperature), but are smaller when $n < 0$. This implies that the flow will become less susceptible to the vortex instability as the value of $n$ increases. This is to be expected, because when $n = 0$ there is a step jump in the temperature difference $(T_w - T_\infty) = A$ for all $x$, whereas for $n > 0$ the wall temperature starts with $T_w = T_\infty$ at $x = 0$ and increases with $x$, and for $n < 0$ it starts with $T_w \to \infty$ at $x = 0$ and decreases with $x$. Thus, for $n < 0$ larger jumps in $(T_w - T_\infty)$ occur at small $x$ than for $n = 0$, which contributes to an earlier onset of the instability and hence a smaller critical $Gr_x/Re_x^{3/2}$ value. This same trend was also observed in refs. [11, 12]. Also included in Table 1 are the $-\theta'(0)$ and $f''(0)$ values. For a given $Pr$, a larger value of the exponent $n$ is seen to provide a larger local Nusselt number due to the larger $-\theta'(0)$ value.

The effect of the exponent $n$ on the critical values of $Gr_x/Re_x^{3/2}$ as a function of Prandtl number is illustrated in Fig. 8. It is interesting to observe from Fig. 8 that for a given value of the exponent $n$ the critical $Gr_x/Re_x^{3/2}$ value increases with increasing Prandtl number until $Pr \approx 100$ and then becomes almost a constant, finite value when the Prandtl number is larger than 100.

In Table 2 the critical values of $Gr_x/Re_x^{3/2}$, $G^*$, and the critical wave number, $\alpha^*$, from the present analysis for the case of $n = 0$ (uniform wall temperature) are compared with results from the previous studies by others. Owing to some numerical errors in the work of Wu and Cheng [1], as pointed out by Moutsoglou *et al.* [2], the accuracy of the results from ref. [1] is subject to question. The results from ref. [2] were based on the parallel flow model in which the amplitude functions of the disturbances are assumed to be independent of the streamwise coordinate. The predicted critical values of $Gr_x/Re_x^{3/2}$ from ref. [2] are about two orders of magnitude lower than those from the experiments by Gilpin *et al.* [6], Moharreri *et al.* [9], and Hayashi *et al.* [13].

Table 1. Numerical results for critical values $G^* = (Gr_x/Re_x^{3/2})^*$, $\alpha^*$ and $-\theta'(0)$

| | $Pr = 0.7$ | | | $Pr = 7$ | | | $Pr = 10^2$ | | | $Pr = 10^3$ | | | $Pr = 10^4$ | | |
|---|---|---|---|---|---|---|---|---|---|---|---|---|---|---|---|
| $n$ | $G^*$ | $\alpha^*$ | $-\theta'(0)$ | $G^*$ | $\alpha^*$ | $-\theta'(0)$ | $G^*$ | $\alpha^*$ | $-\theta'(0)$ | $G^*$ | $\alpha^*$ | $-\theta'(0)$ | $G^*$ | $\alpha^*$ | $-\theta'(0)$ |
| 1.0 | 6.8730 | 0.58434 | 0.48034 | 9.5394 | 0.67547 | 1.04362 | 13.380 | 2.1335 | 2.5347 | 13.609 | 4.7023 | 5.4618 | 13.658 | 10.149 | 11.774 |
| 0.8 | 6.4294 | 0.59728 | 0.45329 | 8.6024 | 0.67639 | 0.98615 | 12.481 | 2.1089 | 2.3955 | 12.704 | 4.6347 | 5.1619 | 12.750 | 10.005 | 11.127 |
| 0.5 | 5.2959 | 0.56774 | 0.40590 | 7.4243 | 0.63904 | 0.88562 | 11.027 | 2.0531 | 2.1520 | 11.243 | 4.5214 | 4.6374 | 11.283 | 9.7629 | 9.9957 |
| 0.2 | 4.6620 | 0.55593 | 0.34557 | 5.7232 | 0.58644 | 0.75791 | 9.3980 | 1.9827 | 1.8429 | 9.6053 | 4.3806 | 3.9713 | 9.6404 | 9.4604 | 8.5597 |
| 0 | 4.2556 | 0.52183 | 0.29268 | 4.8184 | 0.56796 | 0.64593 | 8.1631 | 1.9235 | 1.5719 | 8.3628 | 4.2627 | 3.3875 | 8.3941 | 9.2089 | 7.3014 |
| −0.2 | 2.7737 | 0.49522 | 0.22004 | 3.2740 | 0.54486 | 0.49134 | 6.7381 | 1.8492 | 1.1976 | 6.9266 | 4.1157 | 2.5813 | 6.9537 | 8.8958 | 5.5641 |
| −0.5 | 1.9853 | 0.45637 | 1.32E-05 | 2.0241 | 0.51124 | 1.51E-05 | 3.9221 | 1.6881 | 3.36E-05 | 4.0704 | 3.8090 | 3.45E-04 | 4.0881 | 8.2320 | 3.46E-03 |

Note: $f''(0) = 0.332058$ for Blasius flow, $E\text{-}0x = 10^{-x}$.

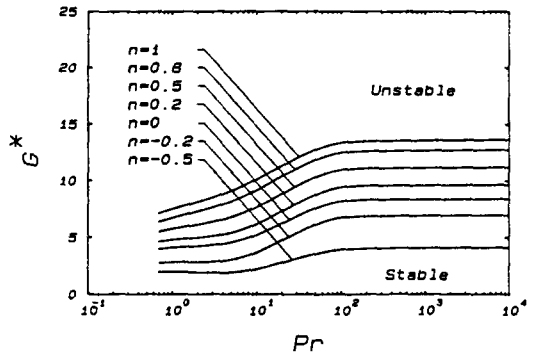


FIG. 8. Critical values of $G^* = (Gr_x/Re_x^{1.5})^*$ for $0.7 \leqslant Pr \leqslant 10^4$ and $-0.5 \leqslant n \leqslant 1.0$.

The critical $Gr_x/Re_x^{3/2}$ values from the present analysis for the UWT case ($n = 0$) are 8.163, 8.363, and 8.394 for $Pr = 10^2$, $10^3$, and $10^4$, respectively. This is in contrast to the value of 7.797 obtained by Yoo *et al.* [4] by power series solution for $Pr \to \infty$. The present analysis is not limited to large Prandtl numbers and the present results are believed to be more accurate. Also, the present critical wave number $\alpha^*$ can be related to the critical wave number $\tilde{\alpha}^*$ based on the thermal boundary layer thickness $\delta_t$, as employed in ref. [4], by

$$\alpha^* = \tilde{\alpha}^* Pr^{1/3}/4.64 \tag{47}$$

where the constant 4.64 comes from the coefficient of the momentum thickness $\delta_m/x = 4.64 Re_x^{-1/2}$ [14] and $\delta_m \doteq Pr^{1/3}\,\delta_t$. It appears that $\alpha^* \to \infty$ when $Pr \to \infty$. However, for large Prandtl numbers, say, $Pr = 10^2$, $10^3$, and $10^4$, the critical wave numbers from the present calculations for the $n = 0$ case in terms of $\tilde{\alpha}^*$ are respectively 1.923, 1.978, and 1.983. Thus, this trend in the change of $\tilde{\alpha}^*$ with increasing $Pr$ agrees well with the calculated value of 1.98 by Yoo *et al.* [4] for $Pr \to \infty$.

The results of Chen and Chen [3] for the UWT case provide the critical values of $Gr_x/Re_x^{3/2} = 7.78$–$8.13$ and $\tilde{\alpha}^* = 1.97$ for $Pr = 1$–$\infty$, which are generally in good agreement with the present results.

It is important to note that for a given value of the exponent $n$ both the critical values of $Gr_x/Re_x^{3/2}$ and the corresponding critical wave number $\alpha^*$ increase with an increase in the Prandtl number. However, the critical $Gr_x/Re_x^{3/2}$ value approaches a finite value when the Prandtl number becomes larger than 100 (see Fig. 8). In addition, for a given Prandtl number $Pr$, a larger value of the exponent $n$ provides a larger critical $Gr_x/Re_x^{3/2}$ value.

From a comparison between the results from the present analysis and that of Moutsoglou *et al.* [2], it is apparent that an accounting of the streamwise dependence of the disturbance amplitude functions reduces the susceptibility of the flow to the vortex mode of instability. From Table 2 one can see that the critical values of $Gr_x/Re_x^{3/2}$ for $Pr = 0.7$ and 7 from the present analysis increase by about one order of magnitude when compared with the results of ref. [2], thus bringing the predicted values to one order closer to the experimental values for air and water as given in refs. [6, 9, 13]. The discrepancy in the results between the linear theory and experiment seems reasonable because natural disturbances in a boundary layer flow need to be amplified before they can be detected, whereas the present prediction is based on the linear theory in which the disturbance quantities are assumed to be infinitesimally small.

Table 2. Comparison of critical values of $G^* = (Gr_x/Re_x^{3/2})^*$, $n = 0$ (UWT)

| Reference | Main flow | Model | $Pr$ | $G^*$ | $\alpha^*$ |
|---|---|---|---|---|---|
| Wu and Cheng [1] (1976) | forced convection | parallel flow | 0.7 | 292.5 | 0.11 |
| | | | 10 | 75.48 | 1.72 |
| | | | $10^2$ | 13.46 | 2.95 |
| | | | $10^3$ | 2.406 | 3.90 |
| | | | $10^4$ | 1.816 | 7.2 |
| Moutsoglou *et al.* [2] (1981) | mixed convection | parallel flow | 0.7 | 0.447 | 0.001–0.060 |
| | | | 7 | 0.434 | 0.0008–0.036 |
| Chen and Chen [3] (1984) | forced convection | non-parallel flow | 1–$\infty$ | 7.78–8.13 | 0.425–$\infty$ |
| Yoo *et al.* [4] (1987) | forced convection | non-parallel flow | $\infty$ | 7.797 | $\infty$ ($\tilde{\alpha}^* = 1.98$) |
| Present analysis | forced convection | non-parallel flow | 0.7 | 4.2556 | 0.52183 |
| | | | 7 | 4.8184 | 0.56796 |
| | | | 30 | 7.6285 | 1.1691 |
| | | | 50 | 7.9400 | 1.4729 |
| | | | $10^2$ | 8.1631 | 1.9235 |
| | | | $10^3$ | 8.3628 | 4.2627 |
| | | | $10^4$ | 8.3941 | 9.2089 |
| Hayashi *et al.* [13] (1977) | forced convection | experiment | 0.7 (air) | 192 | — |
| Gilpin *et al.* [6] (1978) | forced convection | experiment | ~7 (water) | 46–110 | 0.895–2.049 |
| Moharreri *et al.* [9] (1988) | mixed convection | experiment | 0.7 (air) | ~100 | — |

As a final note, it is mentioned here that solutions of equations (33)–(36) by the local similarity method, with terms containing $X\ \partial/\partial X$ in these equations deleted, have provided critical values of $G^* = (Gr_x/Re_x^{3/2})^*$ that are smaller than those from solutions of equations (39)–(41). For example, for $Pr = 0.7$ the value of $G^*$ from the local similarity solution varies from 1.7525 to 2.9620 to 4.1664 as the value of the exponent $n$ is increased from $-0.5$ to 0 to 1.0. This is in contrast to the values of $G^*$ of 1.9853 to 4.2556 to 6.8730 listed in Table 1 from solutions of the 'untruncated' equations (39)–(41). The corresponding critical $G^*$ values for $Pr = 100$ with $n = -0.5$, 0, and 1.0 are 0.2804, 0.5986, and 1.0702, as compared to 3.9221, 8.1631, and 13.380 from Table 1. Thus, the local similarity solution yields a critical $G^*$ value that decreases with increasing Prandtl number $Pr$ for a given value of $n$. This trend is opposite to that from solutions of equations (39)–(41), which shows that $G^*$ increases with increasing $Pr$.

## CONCLUSION

In this paper, thermal instability of forced convection in laminar boundary layer flow over a heated horizontal flat plate with power-law variation in the surface temperature has been investigated analytically using the non-parallel flow model. Neutral stability curves as well as the critical values for $Gr_x/Re_x^{3/2}$ and the corresponding critical wave numbers are presented for Prandtl numbers $0.7 \leqslant Pr \leqslant 10^4$ covering exponent values $-0.5 \leqslant n \leqslant 1.0$. The major findings from the present study can be summarized as follows.

(1) For the power-law variation in the wall temperature, the critical value of $Gr_x/Re_x^{3/2}$ and the corresponding critical wave number $\alpha^*$ both increase with increasing value of the exponent $n$ for a given value of the Prandtl number $Pr$.

(2) For a given value of the exponent $n$, the critical values of $Gr_x/Re_x^{3/2}$ and $\alpha^*$ both increase with increasing value of the Prandtl number $Pr$. However, the critical $Gr_x/Re_x^{3/2}$ value approaches a finite, constant value when the Prandtl number $Pr$ increases to a value larger than 100.

(3) The more rigorous analysis by the non-parallel flow model in the present study provides a larger critical $Gr_x/Re_x^{3/2}$ value than the previous analysis by the parallel flow model.

*Acknowledgement*—Part of the numerical results reported in this paper was obtained by using a CRAY X-MP Supercomputer through the facility of the National Center for Supercomputing Applications (NCSA) at the University of Illinois.

## REFERENCES

1. R. S. Wu and K. C. Cheng, Thermal instability of Blasius flow along horizontal plates, *Int. J. Heat Mass Transfer* **19**, 907–913 (1976).
2. A. Moutsoglou, T. S. Chen and K. C. Cheng, Vortex instability of mixed convection flow over a horizontal flat plate, *J. Heat Transfer* **103**, 257–261 (1981).
3. K. Chen and M. M. Chen, Thermal instability of forced convection boundary layers, *J. Heat Transfer* **106**, 284–289 (1984).
4. J. Y. Yoo, P. Park, C. K. Choi and S. T. Ro, An analysis on the thermal instability of forced convection flow over isothermal horizontal flat plate, *Int. J. Heat Mass Transfer* **30**, 927–935 (1987).
5. S. L. Lee, T. S. Chen and B. F. Armaly, New finite difference solution methods for wave instability problems, *Numer. Heat Transfer* **10**, 1–18 (1986).
6. R. R. Gilpin, H. Imura and K. C. Cheng, Experiments on the onset of longitudinal vortices in horizontal Blasius flow heated from below, *J. Heat Transfer* **100**, 71–77 (1978).
7. E. M. Sparrow and R. B. Husar, Longitudinal vortices in natural convection flow on inclined surfaces, *J. Fluid Mech.* **37**, 251–255 (1969).
8. H. I. Abu-Mulaweh, B. F. Armaly and T. S. Chen, Instabilities of mixed convection flows adjacent to inclined plates, *J. Heat Transfer* **109**, 1031–1033 (1987).
9. S. S. Moharreri, B. F. Armaly and T. S. Chen, Measurements in the transition vortex flow regime of mixed convection above a horizontal heated plate, *J. Heat Transfer* **110**, 358–365 (1988).
10. S. E. Haaland and E. M. Sparrow, Vortex instability of natural convection flow on inclined surfaces, *Int. J. Heat Mass Transfer* **16**, 2355–2367 (1973).
11. C. T. Hsu, P. Cheng and G. M. Homsy, Instability of free convection flow over a horizontal impermeable surface in a porous medium, *Int. J. Heat Mass Transfer* **21**, 1221–1228 (1978).
12. C. T. Hsu and P. Cheng, Vortex instability in buoyancy-induced flow over inclined heated surfaces in porous media, *J. Heat Transfer* **101**, 660–665 (1979).
13. Y. Hayashi, A. Takimoto and K. Hori, Heat transfer in laminar mixed convection flow over a horizontal flat plate (in Japanese), *Proc. 14th Japan Heat Transfer Symp.*, pp. 4–6 (1977).
14. W. M. Kays and M. E. Crawford, *Convective Heat and Mass Transfer* (2nd Edn), Chap. 7. McGraw-Hill, New York (1980).

## INSTABILITE THERMIQUE DE LA CONVECTION FORCEE SUR UNE PLAQUE PLANE HORIZONTALE, CHAUDE, NON ISOTHERME

**Résumé**—Un modèle linéaire à écoulement non parallèle est utilisé pour étudier l'apparition de l'instabilité tourbillonnaire longitudinale dans l'écoulement forcé laminaire pariétale variable selon $T_w(x)-T_\infty = Ax^n$. Dans cette analyse, la dépendance des fonctions d'amplitude de perturbation est prise en compte. Le système résultant d'équations linéarisées pour les fonctions d'amplitude constitue un problème aux valeurs propres qui est résolu par un schéma aux différences finies avec la méthode de tri de Müller. Les courbes de stabilité neutre ainsi que les valeurs critiques de $Gr_x/Re_x^{3/2}$ et les nombres de Prandtl $0{,}7 \leqslant Pr \leqslant 10^4$ avec un domaine d'exposant $-0{,}5 \leqslant n \leqslant 1{,}0$. Pour un nombre de Prandtl donné, l'instabilité thermique décroit lorsque l'exposant $n$ augmente. Pour une valeur donnée de $n$, les fluides à grand nombre de Prandtl montrent moins de sensibilité aux instabilités que des fluides à faible nombre de Prandtl. Cette tendance existe pour $Pr \leqslant 100$. Pour $Pr > 100$, les valeurs critiques de $Gr_x/Re_x^{3/2}$ deviennent constantes et indépendantes du nombre de Prandtl. L'analyse à écoulement non parallèle qui tient compte de la dépendance des fonctions d'amplitude a un effet stabilisant par rapport à l'analyse à écoulement parallèle dans laquelle on néglige cette dépendance.

## DIE THERMISCHE INSTABILITÄT EINER ERZWUNGENEN KONVEKTIONSSTRÖMUNG ÜBER EINE BEHEIZTE, NICHT ISOTHERME WAAGERECHTE EBENE PLATTE

**Zusammenfassung**—Mit Hilfe eines linearen Modells für nicht-parallele Strömung wird das Einsetzen der Längswirbel-Instabilität in laminarer erzwungener Konvektionsströmung über eine beheizte horizontale ebene Platte bei variabler Oberflächentemperatur ($T_w(x)-T_\infty = Ax^n$) untersucht. Dabei wird die Abhängigkeit der Störungsamplituden-Funktionen in Strömungsrichtung berücksichtigt. Es ergibt sich ein System von linearisierten Störungsgleichungen für die Amplituden-Funktionen, das ein Eigenwertproblem darstellt. Dieses wird mit Hilfe eines Finite-Differenzen-Verfahrens unter Verwendung des Zufallsverfahrens nach Müller gelöst. Es werden die Kurven neutraler Stabilität berechnet, außerdem die kritischen Werte für $Gr_x/Re_x^{3/2}$ und die entsprechende kritische Wellenzahl $\alpha^*$ (Prandtl-Zahl: $0{,}7 \leqslant Pr \leqslant 10^4$; Exponent: $-0{,}5 \leqslant n \leqslant 1{,}0$). Es zeigt sich, daß bei gegebener Prandtl-Zahl die thermische Instabilität mit steigenden Exponenten abnimmt. Für einen gegebenen Wert des Exponenten $n$ sind Fluide mit großer Prandtl-Zahl weniger anfällig für die Instabilität als Fluide mit kleiner Prandtl-Zahl. Dieser Trend gilt für $Pr \leqslant 100$. Für $Pr > 100$ wird der kritische Wert von $Gr_x/Re_x^{3/2}$ im wesentlichen konstant und unabhängig von der Prandtl-Zahl. Die Ergebnisse der hier vorgestellten Untersuchung werden mit verfügbaren analytischen und experimentellen Ergebnissen aus früheren Studien verglichen. Dabei zeigt sich, daß die Berücksichtigung der Amplituden-Funktionen einen stabilisierenden Einfluß hat.

## ТЕПЛОВАЯ НЕУСТОЙЧИВОСТЬ ВЫНУЖДЕННОГО КОНВЕКТИВНОГО ТЕЧЕНИЯ НАД НАГРЕТОЙ НЕИЗОТЕРМИЧЕСКОЙ ГОРИЗОНТАЛЬНОЙ ПЛОСКОЙ ПЛАСТИНОЙ

**Аннотация**—Линейная модель непараллельного течения используется для исследования возникновения продольной вихревой неустойчивости при ламинарном вынужденном конвективном течении над нагретой горизонтальной плоской пластиной с переменной температурой поверхности, $T_w(x) - T_\infty = Ax^n$. При анализе учитывается зависимость функций амплитуды колебаний от направления течения. Полученная система линеаризованных уравнений возмущения для амплитудных функций представляет собой задачу на собственные значения, решаемую с использованием конечно-разностной схемы и метода пристрелки по Мюллеру. Нейтральные кривые устойчивости, а также критические значения $Gr_x/Re_x^{3/2}$ и соответствующие критические волновые числа $\alpha^*$ представлены для значений числа Прандтля $0{,}7 \leqslant Pr \leqslant 10^4$ в диапазоне значений показателя степени $-0{,}5 \leqslant n \leqslant 1{,}0$. Обнаружено, что при фиксированном значении числа Прандтля тепловая неустойчивость уменьшается с ростом показателя степени $n$. Причем при данном значении показателя степени $n$ жидкости с высокими числами Прандтля проявляют меньшую восприимчивость к неустойчивости, чем жидкости с низкими числами Прандтля. Однако эта тенденция существует при $Pr \leqslant 100$. Когда $Pr > 100$, критические значения $Gr_x/Re_x^{3/2}$ становятся существенно постоянными и не зависят от числа Прандтля. Результаты проведенного анализа непараллельного течения сравниваются с имеющимися аналитическими и экспериментальными данными предыдущих исследований. Найдено, что при анализе непараллельного течения, учтывающем завимость амплитудных функций от направления потока, проявляется стабилизирующий эффект, отсутствующий при анализе с помощью модели непараллельного течения, в котором данной зависимостью пренебрегают.